Received: 2 March 2023 | Accepted: 8 March 2023

DOI: 10.1002/qre.3324

RESEARCH ARTICLE

WILEY

Design of adaptive EWMA control charts using the conditional false alarm rate

Burcu Aytaçoğlu[1] | **Anne R. Driscoll**[2] | **William H. Woodall**[2]

[1]Department of Statistics, Ege University, Izmir, Turkey

[2]Department of Statistics, Virginia Tech, Blacksburg, Virginia, USA

Correspondence
Anne R. Driscoll, Department of Statistics, Virginia Tech, Blacksburg, VA, USA.
Email: adriscoll@vt.edu

Abstract

Dynamic control limits can be useful in designing control charts, especially when sample sizes, risk scores, or other covariate values change over time. Computer simulation can be used to control the conditional false alarm rate and thus the in-control run length properties. We show that this approach can be useful in designing adaptive exponentially weighted moving average (AEWMA) control charts for which the control chart smoothing parameter at a given time point depends on the observed value at that time point. We use AEWMA charts as examples, but the approach can be applied to the adaptive cumulative sum (CUSUM) chart and other types of adaptive charts.

KEYWORDS

dynamic control limits, exponentially weighted moving average (EWMA) chart, statistical process control, statistical process monitoring

1 | INTRODUCTION

Using simulation or other numerical methods to control the conditional false alarm rate (CFAR) has proven very useful in designing control charts, especially when a covariate varies over time. Recent examples accounting for varying sample sizes include Aytaçoğlu and Woodall,[1] who used the CFAR to determine control limits for the cumulative sum (CUSUM) chart for monitoring proportions, and Aytaçoğlu et al.[2] who used this dynamic control limit approach to design the multivariate exponentially weighted moving average (MEWMA) chart. The method also works well for monitoring the risk-adjusted CUSUM chart of Steiner et al.[3] for which the risk factors vary over time, as demonstrated by Zhang and Woodall.[4] Driscoll et al.[5] gave quite a few other examples of applications.

An area that has yet to be explored is the application of the CFAR approach when designing adaptive control charts. Adaptive control charts have been proposed in the literature for monitoring situations where control chart parameters, the sampling interval, or the sample size at a given time depend on the observed data. Psarakis[6] and Tsung and Wang[7] provided literature reviews of adaptive control charting, while Perdikis and Psarakis[8] focused on recent developments in multivariate adaptive control charting. These reviews show that a vast amount of research has been devoted to both the design and application of adaptive control charting, but the CFAR approach has not been used to design these adaptive charts. It is important to note this approach is only appropriate for adaptive charts when the chart parameters or the sample size are changing depending on observed results. The CFAR method is not appropriate when the sampling interval changes over time, which necessitates use of the average time to signal metric.

In this paper, we apply the CFAR approach to design the adaptive exponentially weighted moving average (AEWMA) charts proposed by Capizzi and Masarotto[9] It could also be applied to the AEWMA method of Haq et al.[10] These adaptive charts are combinations of both Shewhart charts and EWMA charts by weighting observations based on the size of the current error. It is suitable to design these charts with the CFAR method because these adaptive charts are for scenarios where the EWMA smoothing parameter value at a given time depends on the observed value at that time. The CFAR approach could also be used in designing the adaptive CUSUM chart of Sparks.[11]

In our study, we design the AEWMA chart by ensuring that the CFARs are controlled at each time point of monitoring. In Section 2, we define the CFAR. In Section 3, we present the AEWMA method. The simulation algorithm for determining dynamic probability control limits (DPCLs) is given in Section 4. In Section 5, the performance of the AEWMA charts with controlled CFARs for static and dynamic scenarios is discussed. Lastly, conclusions are provided in Section 6.

2 | CONDITIONAL FALSE ALARM RATE

The CFAR is the probability of a false alarm at a given time point conditional on no prior false alarm. The CFAR approach can be used to determine all values of the control limits prior to the start of monitoring for the basic adaptive control charts if we assume that the in-control distribution of the variable(s) being monitored is known along with the in-control parameters. This case is referred to as an example of the static scenario. We also consider the case where the sample size varies and become available only during monitoring. Thus the limits are determined at each time period after this information becomes available. Under this dynamic scenario, the CFAR-based control limits will vary over time and are determined sample-by-sample after the covariate information is obtained.

The static scenario was originally considered by Margavio et al.[12] while methods for the dynamic scenario were first proposed by Shen et al.[13] who proposed dynamic control limits for the EWMA chart when monitoring Poisson count data when the area of opportunity changes over time. An important advantage of this approach is that there is no need to specify a model for the areas of opportunity.

Generally, if one specifies the CFAR to remain constant at a value of α, then the use of the dynamic control limits will yield a geometrically distributed in-control run length distribution with an average run length (ARL) of $1/\alpha$. Here the ARL is defined as the expected number of samples until the chart gives an out-of-control signal.

3 | THE ADAPTIVE EWMA CONTROL CHARTS

One form of the adaptive EWMA chart studied by Capizzi and Masarotto[9] and Haq et al.[10] uses a score function to weight past data. This AEWMA statistic takes the form

$$x_t = x_{t-1} + \phi(e_t),\ x_0 = \eta_0,\ t = 1, 2, \ldots \tag{1}$$

where $e_t = y_t - x_{t-1}, y_t$ is the observation at time t, and $\phi(e_t)$ is a score function. The chart will signal when $|x_t - \eta_0| > h$, where η_0 is the target value of the process mean and h is the selected threshold.

We will use the score function given in Equation (3) of Capizzi and Masarotto[9] to design an AEWMA chart by controlling the CFAR. The score function inspired by Huber's function (Huber[14]) is

$$\phi_t(e_t) = \begin{cases} e_t + (1-\lambda)k & if\ e_t < -k \\ \lambda e_t & if\ |e_t| \le k \\ e_t - (1-\lambda)k & if\ e_t > k \end{cases}, \tag{2}$$

where $0 < \lambda < 1$ and $k \ge 0$. It is important to note that different score functions can be chosen and the CFAR method could be applied similarly.

4 | DYNAMIC PROBABILITY CONTROL LIMITS (DPCLS)

In this study, we will modify the AEWMA presented in Capizzi and Masarotto[9] and Haq et al.[10] by using the DPCLs approach given in Zhang and Woodall.[4] This iterative process was first introduced by Shen et al.,[13] where the idea is to

update the limits at each time point to ensure that the conditional probability of a false alarm given that there have been no previous false alarms is kept constant.

For the AEWMA chart, the DPCLs $h(\alpha) = (h_1(\alpha),\ h_2(\alpha),\ \ldots,\ h_t(\alpha))$ are found such that they satisfy as closely as possible the following equations:

$$\Pr(|x_1| > h_1(\alpha)\,|n_1) = \alpha$$

$$\Pr(|x_t| > h_t(\alpha)\,||x_i| < h_i(\alpha),\ 1 \le i < t,\ n_t) = \alpha \text{ for } t > 1,$$

where α is the prespecified CFAR and $n_1,\ n_2,\ \ldots$, is the sequence of sample sizes. The chart will signal when $|x_t| > h_t(\alpha)$.

The simulation-based procedure for the DPCLs begins at the first time point, $t = 1$. If the process is in-control, then the data values are assumed to be independent and follow a normal distribution with mean $\mu_0 = 0$ and variance $\sigma_0 = 1$. At $t = 1$, n_1 random observations are observed and the sample mean, $\bar{y}_1$, is obtained. In order to obtain the control limit at the first time point, $t = 1$, a number of random samples are generated and the sample means $\bar{y}_{1,i}$ are computed where $i = 1,\ 2,\ \ldots,\ M$. The next step is to calculate the AEMWA statistics $x_{1,1},\ x_{1,2},\ \ldots,\ x_{1,M}$ using Equation (1) and the Huber score function in Equation (2). It is important to note that $x_0 = \eta_0 = 0$ in this example. The absolute value of the M AEWMA statistics are sorted in ascending order $|x|_{1,(1)},\ |x|_{1,(2)},\ldots,\ |x|_{1,(M)}$ and the $M' = M(1-\alpha)$ largest AEWMA statistic $x_{1,(M')}$ is taken as the approximated upper DPCL, $h_1(\alpha)$, and $-h_1(\alpha)$ is taken as the lower DPCL. In practice, after obtaining the control limit $h_1(\alpha)$, the value of the AEWMA statistic $|x_1|$, which is calculated based on the observed $\bar{y}_1$, would be compared with $h_1(\alpha)$. If $|x_1| > h_1(\alpha)$, the chart signals. Otherwise, we proceed to the next time point $t = 2$.

Then, for $t = 2$, M normal random samples with a mean 0 and variance 1 are generated and $\bar{y}_{2,i}$ are calculated. Again, the corresponding AEWMA statistics $x_{2,i},\ i = 1,\ 2,\ \ldots, M$ are obtained using Equation (1) and the score function found in Equation (2). It is important to note that the value $x_{1,i}$ is needed to compute both $e_{2,i}$ and $x_{2,i}$. The value for $x_{1,i}$ is randomly chosen with replacement from step one with the requirement that $|x_{1,i}| < h_1(\alpha)$. Afterwards, the absolute value of the M values of $|x|_{2,i}$ are sorted in ascending order and the upper α percentile $x_{2,(M')}$ is taken as the upper DPCL $h_2(\alpha)$ and correspondingly $-h_2(\alpha)$ for the lower DPCL. For the next time point, the AEWMA statistics that are less than or equal to $h_2(\alpha)$ and greater than or equal to $-h_2(\alpha)$ are stored and the same procedure is repeated in order to obtain $h_3(\alpha)$ and $-h_3(\alpha)$. This process is continued iteratively to obtain the remaining control limits. The algorithm for this simulation based procedure is given as follows:

1. Generate M normal random samples with mean $\mu_0 = 0$ and variance $\sigma_0 = 1$ and compute the M sample means, $\bar{y}_{t,i}$ *(i = 1, 2,…,M)*.
2. Compute $e_{t,i} = \bar{y}_{t,i} - x_{t-1,i}$. While computing $e_{t,i}$ randomly choose $x_{t-1,i}$ with replacement from the previous step but only if $|x_{t-1,i}| \le h_{t-1}(\alpha)$.
3. Compute the score function $\phi_{t,i}$ *(i = 1, 2,…,M)*

$$\phi_{t,i}(e_{t,i}) = \begin{cases} e_{t,i} + (1-\lambda)k \ if\ e_{t,i} < -k \\ \lambda e_{t,i} \ if\ |e_{t,i}| \le k \\ e_{t,i} - (1-\lambda)k \ if\ e_{t,i} > k \end{cases}.$$

4. Calculate the AEWMA statistics $x_{t,i} = x_{t-1,i} + \phi_{t,i}(e_{t,i})$ *(i = 1, 2,…,M)* where $x_{t-1,i}$ was randomly chosen with replacement from the previous step but only if $|x_{t-1,i}| \le h_{t-1}(\alpha)$, that is, the value obtained in step 2.
5. Sort the absolute values of M AEWMA statistics, $x_{t,i}$ *(i = 1, 2,…,M)*, in ascending order and take the upper α percentile, $x_{t,(M')}$ where $M' = M(1-\alpha)$ of those M values as the approximated upper DPCL $h_t(\alpha)$, and its negative as the lower DPCL, $-h_t(\alpha)$.

5 | NUMERICAL RESULTS

The performance for the AEWMA chart with DPCLs will be evaluated for charts presented in Capizzi and Masarotto.[9] For these charts, we will study both static and dynamic scenarios. For all simulations, the CFAR was controlled to be approximately $\alpha = 0.002$, where $T = 200$, the number of time points for which DPCLs are calculated. As stated previously, the use of the DPCLs results in a run length distribution that is approximately geometrically distributed. Therefore, the

TABLE 1 AEWMA chart parameters from Table III in Capizzi and Masarotto.[9]

Scenario	λ	k	h
1	0.1253	2.7765	0.8238
2	0.0137	3.4473	0.1835

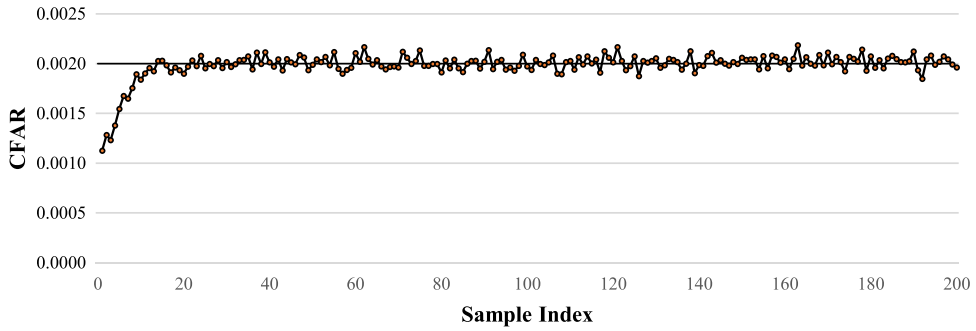

FIGURE 1 Estimated CFARs for the AEWMA chart based on a constant control limit with $h = 0.8238$ ($\lambda = 0.1253$, $k = 2.7765$, $n = 1$).

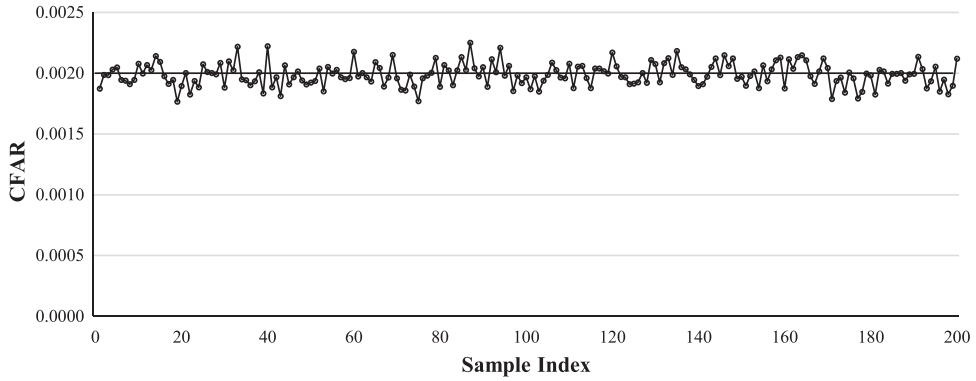

FIGURE 2 Estimated CFARs for the AEWMA chart with DPCLs ($\lambda = 0.1253$, $k = 2.7765$, $n = 1$). rol limits.

in-control ARL values for the charts are approximately 500. For each step of the DPCL algorithm, we generated $M = 500,000$ normal random samples and determined the DPCLs. To determine chart performance, we simulated 10,000 charts with the given limits until each signaled. For every chart we calculated an estimate of the in-control ARL ($\widehat{ARL}_0$), the in-control standard deviation of the run length ($\widehat{SDRL}_0$), and the 10th, 25th, 50th, 75th, and 90th percentiles of the in-control run length distribution ($Q_{0.10}, Q_{0.25}, Q_{0.50}, Q_{0.75}, Q_{0.90}$).

5.1 | CFAR comparisons

The CFAR can be estimated at each time point by calculating the number of AEWMA statistics which are greater than $h_t(\alpha)$ and less than $-h_t(\alpha)$, and dividing by M, the number of random observations generated. In order to illustrate the AEWMA approach based on DPCLs that control the CFAR, two different AEWMA charts were designed using parameters suggested in Capizzi and Masarotto.[9] Table 1 gives the chart parameters from Table III in Capizzi and Masarotto[9] for the AEWMA charts chosen here to illustrate the design of the AEWMA chart. For both scenario 1 and 2, the sample size is constant with $n = 1$.

The CFARs are given in Figure 1 for scenario 1 with the constant control limit ($h = 0.8238$) as suggested in Capizzi and Masarotto.[9] Initially, the CFAR values are below the desired 0.002 value, illustrating that when a constant control limit is used, the CFAR is not constant across all time points. In contrast, Figure 2 shows the CFAR for the AEWMA chart designed using DPCLs that control the CFAR. As expected, the CFAR remains at 0.002 with some random error around

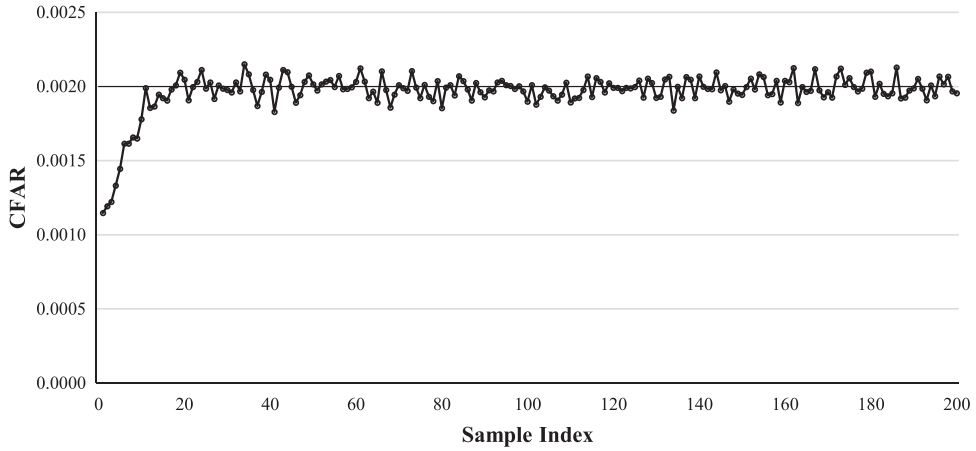

FIGURE 3 Estimated CFARs for the AEWMA chart based on a constant control limit with $h = 0.1835$ ($\lambda = 0.0137$, $k = 3.4473$, $n = 1$).

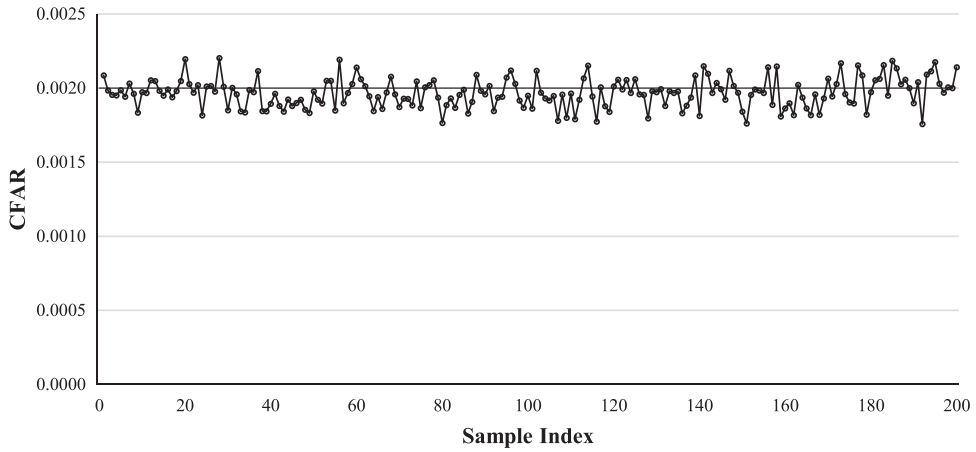

FIGURE 4 Estimated CFARs for the AEWMA chart with DPCLs ($\lambda = 0.0137$, $k = 3.4473$, $n = 1$).

that value. These same results are depicted in Figures 3 and 4 for the scenario 2 design parameters illustrating that the CFAR for the AEWMA chart with DPCL limits can be controlled for different values of λ and k.

5.2 | AEWMA with DPCLS performance

The AEWMA performance for scenarios 1 and 2 given in Table 1 are presented in Table 2. Both static and dynamic situations were studied. The performance for the static scenarios is summarized in Table 2 for AEWMA charts where $n = 1, 5$, and 8. The simulation algorithm discussed in Section 4 was used where the CFAR was set to 0.002. Because the sample size remains constant, the control limits could be determined prior to monitoring. The distribution of the run length for all three cases closely resembles that of the geometric distribution, which is expected for our method based on controlling the CFARs. We also note that the first row for each scenario in Table 2 summarizes the performance of the AEWMA chart with constant control limits. The run lengths for AEWMA charts with constant limits do not necessarily follow a geometric distribution. This is especially apparent for scenario 2 based on the deviations of the percentiles from that of the theoretical geometric distribution.

The DPCLs are plotted in Figures 5 and 6 for scenarios 1 and 2 when $n = 1$. These plots illustrate how the DPCLs start closer to 0 and then converge to a limiting value. However, the shape of the limits depends on the chart parameters k and λ.

The performance for the AEWMA charts with varying sample sizes are also depicted in Table 2. The first case involves randomly generating sample sizes from a discrete uniform distribution with values from 3 to 7, inclusive, that is, from

TABLE 2 Estimated in-control performance of the AEWMA control chart with different chart parameters and with DPCLs where the sample sizes vary.

Parameters	Sample Size	$\widehat{ARL_0}$	$\widehat{SDRL_0}$	$Q_{0.10}$	$Q_{0.25}$	$Q_{0.50}$	$Q_{0.75}$	$Q_{0.90}$
Scenario 1 $\lambda = 0.1253$ $k = 2.7765$	$n = 1$ ($h = 0.8238$)	499.3	490.4	56	148	347	698	1137
	$n = 1$	493.9	492.6	54	141	344	691	1141
	$n = 5$	496.9	492.8	53	144	347	687	1137
	$n = 8$	507.1	507.7	53	144	354	704	1167
	$n \sim$ DU[3,7]	504.7	501.7	55	146	354	703.3	1160.1
	$n \sim$ DU[6,10]	496.3	496.8	54	140	339	698	1164
	$n \sim$ DU[3,7] → DU[6,10]	499.0	509.0	54	145	336	687	1140
	$n = 8 \rightarrow n = 5$	503.2	501.8	52	145	347	701.3	1156.1
Scenario 2 $\lambda = 0.0137$ $k = 3.4473$	$n = 1$ ($h = 0.1835$)	504.1	477.0	81	170	357	688	1107
	$n = 1$	497.7	497.1	53	146	347	691	1129.1
	$n = 5$	504.5	504.3	54	144	350	701	1154
	$n = 8$	501.7	505.9	57	147	347	694	1134
	$n \sim$ DU[3,7]	500.6	503.1	52.9	142	344	702.3	1139
	$n \sim$ DU[6,10]	501.6	497.3	53	143	357	695	1154
	$n \sim$ DU[3,7] → DU[6,10]	498.9	500.6	52	142	342.5	688	1167.1
	$n = 8 \rightarrow n = 5$	501.7	508.1	55	144	342	692	1153.1
Geometric ($\alpha = 0.002$)		500.0	499.5	52	143	346	692	1150

The first row for each scenario denotes the performance with constant limit, h.

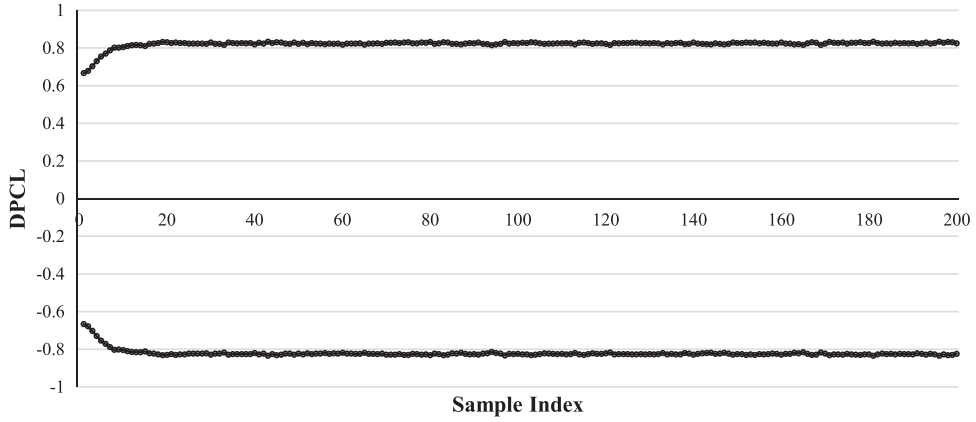

FIGURE 5 DPCLs for the AEWMA chart ($\lambda = 0.1253$, $k = 2.7765$, $n = 1$).

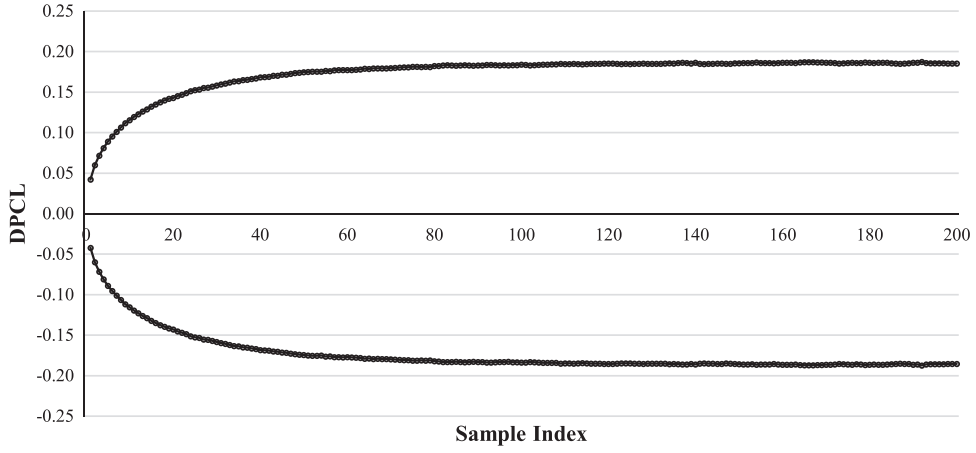

FIGURE 6 DPCLs for the AEWMA chart ($\lambda = 0.0137$, $k = 3.4473$, $n = 1$).

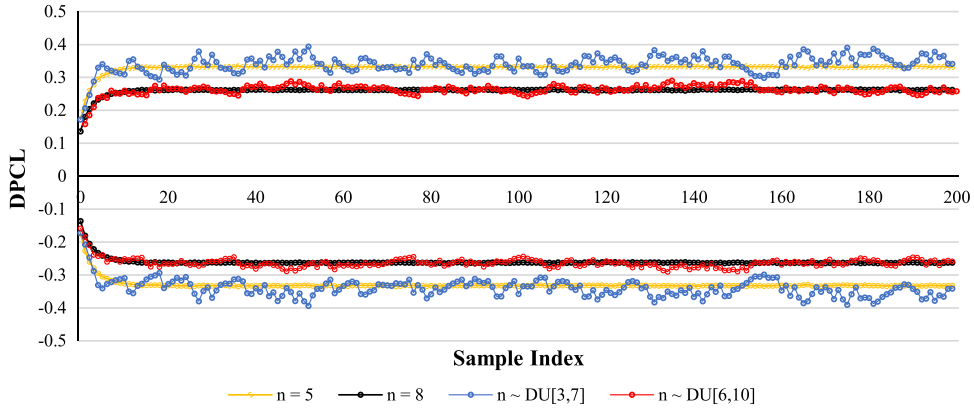

FIGURE 7 DPCLs for the AEWMA chart for different sample size distributions ($\lambda = 0.1253$, $k = 2.7765$).

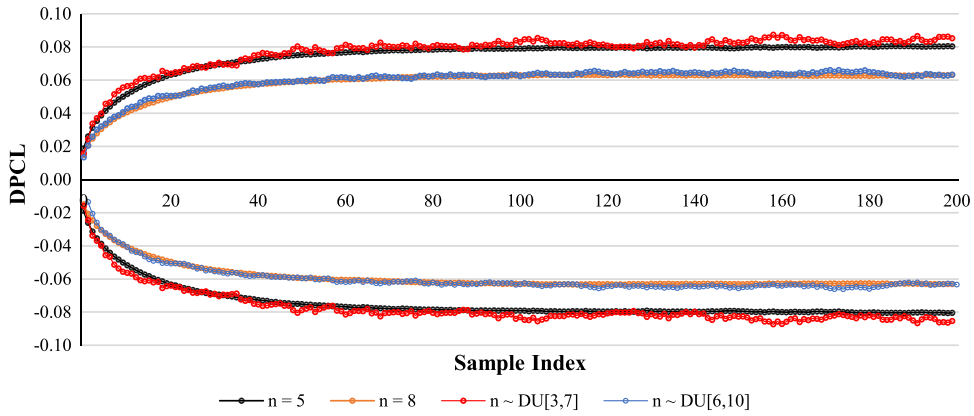

FIGURE 8 DPCLs for the AEWMA chart for different sample size distributions ($\lambda = 0.0137$, $k = 3.4473$).

DU[3,7]. In the second case we generated sample sizes from DU[6, 10]. The next case showed how the method automatically adapts to a change in the sample size distribution. For the first 50 time periods, the sample sizes were generated from DU[3,7], then the distribution shifted to DU[6,10] for later time periods. The last case shows how the chart adapts to a shift in the sample size from $n = 8$ to $n = 5$.

For all dynamic cases, the estimated in-control ARL is approximately 500. Like the static case, the distribution of the in-control run length for all cases very closely resembles the geometric distribution. The DPCLs for $n = 5$ and $n = 8$ along with the cases for $n \sim DU[3, 7]$ and $n \sim DU[6, 10]$ for scenarios 1 and 2 are depicted in Figures 7 and 8, respectively. For all cases, the basic shape of the DPCLs is consistent, but the curves shift depending on the sample size distribution.

The DPCLs can also adapt to a change in sample size during monitoring. Figures 9 and 10 depict the DPCLs for scenario 1 when the sample size shifts from DU[3, 7] to DU[6,10] and when the sample size shifts from $n = 8$ to $n = 5$. For all both cases, the shift occurs after the 50th sample, which is apparent on the plots.

6 | CONCLUSION

We have shown how control of the CFAR can be used to determine the control limits of AEWMA charts. Using the dynamic limits is particularly effective at determining appropriate limits at the initial stage of monitoring, which was noted as a specific point worthy of further investigation by Capizzi and Masarotto.[9] The approach can be used to determine limits with a constant CFAR even if the sample size and/or score function varies over time. The run length performance under all cases studied resembles that of a geometric distribution, which is expected. A major advantage of controlling the CFAR to determine control limits is that no assumptions about the sample size need to be made to design the chart. Our results also have shown how the chart can adapt to changes in the sample size over time. This is just one example of using DPCLs with adaptive control charts. This method could easily be extended to other adaptive control charts.

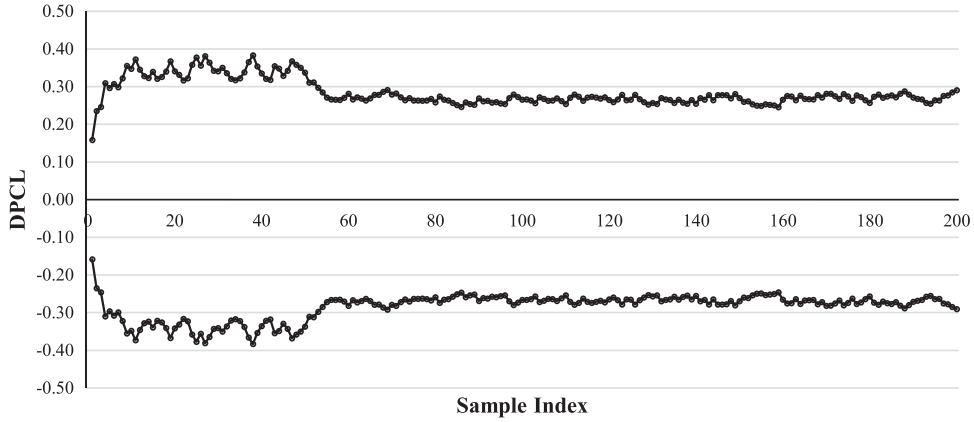

FIGURE 9 DPCLs for the AEWMA chart when sample size distribution shifts from DU[3,7] to DU[6,10] after the 50th sample ($\lambda = 0.1253$, $k = 2.7765$).

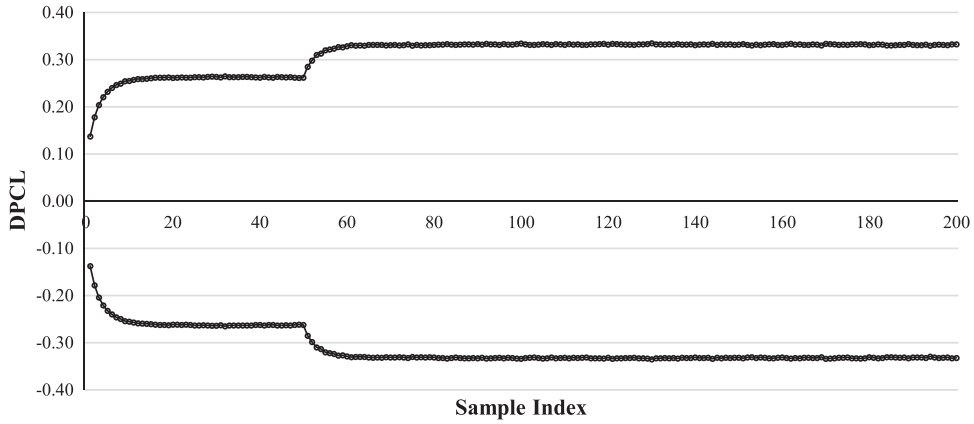

FIGURE 10 DPCLs for the AEWMA chart when sample size shifts from $n = 8$ to $n = 5$ after the 50th sample ($\lambda = 0.1253$, $k = 2.7765$).

DATA AVAILABILITY STATEMENT

We have no data to make available.

ORCID

Burcu Aytaçoğlu https://orcid.org/0000-0002-7164-9240
Anne R. Driscoll https://orcid.org/0000-0003-4308-9570

REFERENCES

1. Aytaçoğlu B, Woodall WH. Dynamic probability control limits for CUSUM charts for monitoring proportions with time-varying sample sizes. *Qual Reliab Eng Int*. 2020;36:592-603.
2. Aytaçoğlu B, Driscoll AR, Woodall WH. Controlling the conditional false alarm rate for the MEWMA control chart. *J Qual Technol*. 2022;54(5):487-502.
3. Steiner SH, Cook RJ, Farewell VT, Treasure T. Monitoring surgical performance using risk-adjusted cumulative sum charts. *Biostatistics*. 2000;1(4):441-452.
4. Zhang X, Woodall WH. Dynamic probability control limits for risk-adjusted Bernoulli CUSUM charts. *Stat Med*. 2015;34(25):3336-3348.
5. Driscoll AR, Woodall WH, Zou C. Use of the conditional false alarm metric in statistical process monitoring. In: Knoth S, Schmid W, eds. *Frontiers in Statistical Quality Control 13*. Springer; 2021:3-12.
6. Psarakis S. Adaptive control charts: recent developments and extensions. *Qual Reliab Eng Int*. 2015;31(7):1265-1280.
7. Tsung F, Wang K. Adaptive charting techniques: literature review and extensions. *Front Statist Qual Control*. 2010; 9:19-35.
8. Perdikis T, Psarakis S. A survey on multivariate adaptive control charts: recent developments and extensions. *Qual Reliab Eng Int*. 2019;35(5):1342-1362.
9. Capizzi G, Masarotto G. An adaptive exponentially weighted moving average control chart. *Technometrics*. 2003;45(3):199-207.

10. Haq A, Gulzar R, Khoo MB. An efficient adaptive EWMA control chart for monitoring the process mean. *Qual Reliab Eng Int*. 2018;34(4):563-571.
11. Sparks RS. CUSUM charts for signalling varying location shifts. *J Qual Technol*. 2000;32(2):157-171.
12. Margavio TM, Conerly MD, Woodall WH, Drake LG. Alarm rates for quality control charts. *Stat Probab Lett*. 1995;24(3):219-224.
13. Shen X, Tsung F, Zou C, Jiang W. Monitoring Poisson count data with probability control limits when sample sizes are time-varying. *Nav Res Logist*. 2013;60(8):625-636.
14. Huber PJ. *Robust Statistics*. Wiley; 1981.

How to cite this article: Aytaçoğlu B, Driscoll AR, Woodall WH. Design of adaptive EWMA control charts using the conditional false alarm rate. *Qual Reliab Engng Int*. 2023;39:2206–2214. https://doi.org/10.1002/qre.3324

AUTHOR BIOGRAPHIES

Dr. Burcu Aytaçoğlu is an assistant professor in the Department of Statistics at Ege University, Izmir, Turkey. She received her BS from the Department of Statistics, Middle East Technical University (METU) and MSc degree both from the Department of Statistics and Department of Industrial Engineering, METU. After working as a production planning engineer in the automotive industry for about 6 years in Izmir, she received her PhD in Statistics from Ege University in 2013. Her research interests are statistical inference, statistical process control, process capability, and control charts.

Dr. Anne R. Driscoll is an Associate Collegiate Professor in the Department of Statistics at Virginia Tech. She received her PhD in Statistics from Virginia Tech. Her research interests include statistical process control, design of experiments, and statistics education. She is a member of ASQ and ASA.

Dr. William H. Woodall is an emeritus professor in the Department of Statistics at Virginia Tech. He is a former editor of the *Journal of Quality Technology* (2001–2003). He is the recipient of the Box Medal (2012), Shewhart Medal (2002), Hunter Award (2019), Youden Prize (1995, 2003), Brumbaugh Award (2000, 2006), Bisgaard Award (2012), Nelson Award (2014), Ott Foundation Award (1987), and best paper award for *IIE Transactions on Quality and Reliability Engineering* (1997). He is a Fellow of the American Statistical Association, a Fellow of the American Society for Quality, and an elected member of the International Statistical Institute.